

# Quantum Yields of Luminescent Lanthanide Chelates and Far-Red Dyes Measured by Resonance Energy Transfer

Ming Xiao and Paul R. Selvin\*

Contribution from the Physics Department and Biophysics Group, University of Illinois, Urbana, Illinois 61801

Received August 23, 2000. Revised Manuscript Received May 14, 2001

**Abstract:** Luminescent lanthanide chelates have unusual spectroscopic characteristics that make them valuable alternative probes to conventional organic fluorophores. However, fundamental parameters such as their quantum yield, and radiative and nonradiative decay rates have been difficult or impossible to measure. We have developed a simple and robust method based on resonance energy transfer to accurately measure these parameters. In addition, the excitation/emission process in lanthanide chelates involves several steps, and we are able to quantify each step. These include excitation of an organic antenna, transfer of energy from the antenna to lanthanide, and then lanthanide emission. Overall, the parameters show that lanthanide chelates can be efficient long-lived emitters, making them sensitive detection reagents and excellent donors in resonance energy transfer. The method is also shown to be applicable to photophysical characterization of red-emitting dyes, which are difficult to characterize by conventional means.

Luminescent lanthanide chelates are valuable alternative probes to conventional fluorophores. The two most useful lanthanides, terbium or europium, have unusual spectroscopic characteristics, including millisecond lifetime, sharply spiked (few nm) emission spectra, and large (> 150 nm) Stokes shifts. These characteristics enable temporal and spectral discrimination against background fluorescence, leading to detection sensitivities of  $10^{-12}$ – $10^{-15}$  M (reviewed in ref 1). These characteristics are also highly beneficial when using lanthanide chelates as donors in fluorescence resonance energy transfer experiments to measure nanometer-scale conformational changes and in homogeneous assays to detect binding events.<sup>2,3</sup>

Many lanthanide chelate complexes have been made,<sup>1</sup> and examples of ones used here and previously<sup>2,4</sup> are shown in Figure 1a. The chelate complex contains several parts, and the excitation/emission process involves several steps (Figure 1b). An organic chromophore acts as an antenna or sensitizer, absorbing excitation light and transferring energy to the lanthanide. This overcomes the inherently weak absorption cross-section of the lanthanide. The excited lanthanide then loses energy either by emitting a photon or producing heat (phonons). The chelate serves several purposes: it provides a scaffold for covalently attaching the antenna in close proximity to the lanthanide, thereby facilitating the transfer of energy from antenna to lanthanide; it displaces water from the primary coordination sphere of the lanthanide, which would otherwise quench the lanthanide luminescence; and it also provides a scaffold for attaching a reactive group (R) for coupling to biomolecules.

\* To whom correspondence should be addressed at: Loomis Laboratory of Physics, University of Illinois, 1110 W. Green St., Urbana, IL 61801. Telephone: 217-244-3371. Fax: 217-244-7187. E-mail: selvin@uiuc.edu.

(1) Sammes, P. G.; Yahioglu, G. *Nat. Prod. Rep.* **1996**, *13*, 1–28 and references therein.

(2) Cha, A.; Snyder, G. E.; Selvin, P. R.; Bezanilla, F. *Nature* **1999**, *402*, 809–813 and references therein.

(3) Mathis, G. *Clin. Chem.* **1995**, *41*, 1391–1397 and references therein.

(4) Li, M.; Selvin, P. R. *J. Am. Chem. Soc.* **1995**, *117*, 8132–8138.

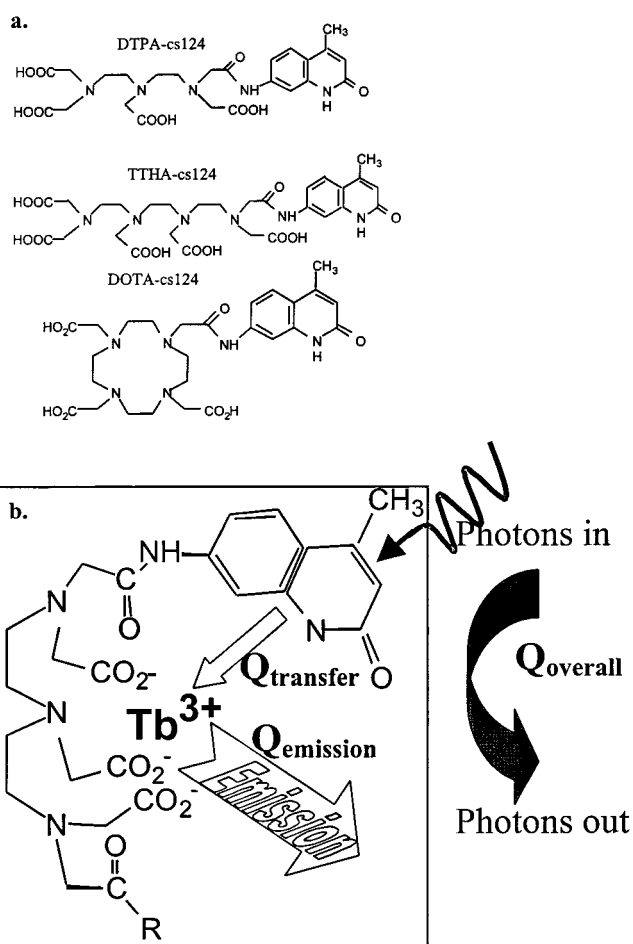


**Figure 1.** (a) Structure of lanthanide chelates. (b) Definition of quantum yields.

Measuring the efficiency of energy transfer from antenna to lanthanide, and then the radiative and nonradiative rates of the

lanthanide excited state, has been difficult or impossible. These parameters, however, are central to understanding the photo-physics of the chelates and in their use in resonance energy transfer measurements (see also Results and Discussion). For example, the brightness ( $B$ ) of the complex is a product of the absorption cross-section of the antenna ( $\epsilon$ ) times the energy transfer efficiency from antenna to lanthanide ( $Q_{\text{transfer}}$ ) times the probability of lanthanide emission once the lanthanide is excited ( $Q_{\text{Ln}}$ ):  $B = \epsilon Q_{\text{transfer}} Q_{\text{Ln}}$

In analogy with conventional fluorophores, the overall quantum yield, can be defined as:

$$Q_{\text{overall}} = Q_{\text{transfer}} Q_{\text{Ln}} \quad (1)$$

That is, the overall quantum yield treats the chelate complex as a "black box" where internal processes are not explicitly considered: given that complex absorbs a photon (i.e., the antenna is excited),  $Q_{\text{overall}}$  is the probability that a lanthanide photon will be emitted.  $Q_{\text{transfer}}$  is the probability that the lanthanide will be excited given that the antenna was excited;  $Q_{\text{Ln}}$  is the probability that a photon will be emitted from the lanthanide, given that the lanthanide was excited.  $Q_{\text{Ln}}$  is related to the radiative ( $k_{\text{rad}}$ ) and nonradiative ( $k_{\text{nr}}$ ) rates:

$$Q_{\text{Ln}} = k_{\text{rad}} / (k_{\text{rad}} + k_{\text{nr}}) = \tau * k_{\text{rad}} \quad (2)$$

where  $\tau$  is the excited-state lifetime of the lanthanide and equals  $(k_{\text{rad}} + k_{\text{nonrad}})^{-1}$ .

In this work we measure  $Q_{\text{overall}}$  and  $\tau$  by standard techniques and report a new method for measuring  $Q_{\text{Ln}}$ . Once  $Q_{\text{Ln}}$  is known,  $Q_{\text{transfer}}$  and  $k_{\text{rad}}$  and  $k_{\text{nr}}$  can then be deduced using eqs 1 and 2. The method for measuring  $Q_{\text{Ln}}$  is simple and robust. It is based on diffusion-enhanced energy transfer,<sup>5</sup> wherein a freely diffusing lanthanide donor transfers energy to an organic acceptor fluorophore with known quantum yield ( $Q_a$ ). By measuring the energy transfer efficiency from lanthanide to acceptor by both lifetime and spectra,  $Q_{\text{Ln}}$  can be readily determined (see Materials and Methods). In addition, once  $Q_{\text{Ln}}$  is known, the experiment can be repeated with another organic acceptor fluorophore whose quantum yield is not known, and  $Q_a$  can then be deduced. This is therefore also a new method for measuring quantum yields of organic fluorophores.

## Materials and Methods

**Overview.** A lanthanide chelate (Figure 1) is mixed with an acceptor of known quantum yield, and the efficiency of energy transfer ( $E$ ) between them is calculated from both lifetime and intensity measurements. By comparing the spectra and lifetime measurements and knowing that they must lead to the same value for  $E$ ,  $Q_{\text{Ln}}$  can be determined from the equations below. Specifically,  $E$  can be calculated from the lifetimes of donor luminescence (eq 3, middle term) or lifetime of the sensitized emission (right-hand term of eq 3), where sensitized emission is the delayed acceptor fluorescence due *only* to energy transfer from the donor.

$$E = 1 - (\tau_{\text{da}}/\tau_{\text{d}}) = 1 - (\tau_{\text{ad}}/\tau_{\text{d}}) \quad (3)$$

$\tau_{\text{da}}$  and  $\tau_{\text{d}}$  are the donor's excited-state lifetime in the presence and absence of the acceptor, respectively, and  $\tau_{\text{ad}}$  is the lifetime of the sensitized emission. (The lifetime of sensitized emission can readily be measured without interference from donor emission or from direct acceptor emission.<sup>6</sup> Donor emission is eliminated by detecting where

the donor is dark; direct acceptor emission is eliminated by time-gating following an excitation pulse since the direct emission is very short (ns) compared to sensitized emission ( $\mu\text{s}$ – $\text{ms}$ .)  $E$  can also be determined by measuring the intensity of sensitized emission ( $I_{\text{ad}}$ ) and comparing it to the residual donor emission in the presence of acceptor ( $I_{\text{da}}$ ):<sup>7</sup>

$$E = (I_{\text{ad}}/Q_a)/(I_{\text{da}}/Q_{\text{Ln}} + I_{\text{ad}}/Q_a) \quad (4)$$

where  $Q_a$  is the quantum yield of the acceptor and  $Q_{\text{Ln}}$  is quantum yield for the lanthanide donor (in the absence of acceptor), as discussed previously.

To understand eq 4, recall that energy transfer,  $E$ , is defined as the number of donor excitations that lead to acceptor excitations, divided by the total number of donor excitations. The numerator in eq 4 is simply the number of excitations of the acceptor due to energy transfer; the denominator is the total number of excitations of the lanthanide donor. The denominator has two parts. Some of the lanthanide donor excitations lead to donor emission without energy transfer; this is the first term,  $I_{\text{da}}/Q_{\text{Ln}}$ . Some of the lanthanide excitations lead to energy transfer and hence acceptor excitation; this is the second term,  $I_{\text{ad}}/Q_a$ .

For calculating  $E$ , eq 4 has advantages over conventional formulas. Specifically, via eq 4, the precision in the measurement of  $E$  (and ultimately in  $Q_{\text{Ln}}$ —see below) is very high because we only compare ratios of intensities measured simultaneously on a single sample instead of comparing intensities of two different samples (e.g., a donor with and without acceptor), as required by conventional methods.

By combining eqs 3 and 4 and using an acceptor of known quantum yield, one can readily calculate  $Q_{\text{Ln}}$  through eq 5.

$$Q_{\text{Ln}} = Q_a \times (I_{\text{da}}/I_{\text{ad}})/(1/E - 1) = Q_a I_{\text{da}}(\tau_{\text{d}} - \tau_{\text{ad}})/(I_{\text{ad}}\tau_{\text{ad}}) \quad (5)$$

After  $Q_{\text{Ln}}$  is determined,  $Q_a$  of an acceptor with an unknown quantum yield can be then determined by rearranging eq 5:

$$Q_a = Q_{\text{Ln}}([1/E] - 1)/(I_{\text{da}}/I_{\text{ad}}) = Q_{\text{Ln}} I_{\text{ad}}\tau_{\text{ad}}/(I_{\text{da}}(\tau_{\text{d}} - \tau_{\text{ad}})) \quad (6)$$

Note that the detailed energy transfer mechanism is unimportant for determining  $E$  and the quantum yields as long as the energy transfer is in the weak coupling limit; that is, the presence of acceptor does not alter the wave function of the donor.

Methodologically, the lanthanide and acceptor could be at a fixed distance from each other, but allowing them to freely diffuse has three benefits. (1) In this "diffusion-enhanced energy transfer" method,<sup>5</sup>  $E$  can be easily varied using different acceptor concentrations, a control to ensure that  $Q_{\text{Ln}}$  is independent of  $E$ . (2) Lifetimes are single exponential in the "rapid diffusion" limit<sup>5</sup> and hence can be measured accurately. (3) Different acceptors can be readily used.

Once  $Q_{\text{Ln}}$  and  $\tau_{\text{d}}$  are measured, radiative ( $k_{\text{rad}}$ ) and nonradiative ( $k_{\text{nr}}$ ) rates for the lanthanide excited state can be determined:

$$k_{\text{rad}} = Q_{\text{Ln}}/\tau_{\text{d}} \quad k_{\text{nr}} = (1 - Q_{\text{Ln}})/\tau_{\text{d}} \quad (7)$$

Finally, with  $Q_{\text{Ln}}$  measured as above and by measuring  $Q_{\text{overall}}$  via conventional methods (comparing the lanthanide brightness to a standard fluorophore of known quantum yield),  $Q_{\text{transfer}}$  can be calculated from eq 1.

**Chemicals.** Diethylenetriaminepentaacetic acid (DTPA)—7-amino-4-methyl-2(1H)-quinolinone (carbonyl 124 [cs124]), triethylenetetraaminehexanoic acid (TTHA)—cs124, and 1,4,7,10-tetraazacyclododecane- $N,N',N'',N'''$ -tetraacetic acid (DOTA)—cs124 were synthesized and labeled with metal as described previously.<sup>4</sup> 5-Carboxy-tetramethylrhodamine and fluorescein were purchased from Molecular Probes, SulfoRhodamine 101 from Exciton, and Cy5-NHS and Cy5.5 NHS (mono) ester from Amersham.

**Sample Preparation for Diffusion-Enhanced Energy Transfer.** Lanthanide chelate complexes were diluted to 1  $\mu\text{M}$  in 25 mM MOPS buffer (pH 7.0) except for energy transfer measurements using fluorescein as acceptor, in which case the lanthanide chelate complexes

(5) Stryer, L.; Thomas, D. D.; Meares, C. F. In *Diffusion-Enhanced Fluorescence Energy Transfer*; Mullins, L. J., Ed.; Annual Reviews, Inc.: Palo Alto, CA, 1982; Vol. 11, pp 203–222.

(6) Selvin, P. R.; Hearst, J. E. *Proc. Natl. Acad. Sci., U.S.A.* **1994**, *91*, 10024–10028.

(7) Selvin, P. R. *IEEE J. Sel. Top. Quantum Electron.* **1996**, *2*, 1077–1087.

were diluted in 25 mM MOPS (pH 8.35). The energy transfer acceptor was added at different final concentrations (in  $\mu\text{M}$  range) to generate different levels of the energy transfer efficiency.

**Spectroscopy.** Lifetime and wavelength emission spectra were recorded on a spectrometer built in our laboratory.<sup>8</sup> Specifically, a solution of the lanthanide chelate and energy transfer acceptor was placed in a 3 mm  $\times$  3 mm quartz cuvette and excited with a pulsed nitrogen laser (337 nm, 5 ns pulse-width, 40 Hz repetition rate). To avoid inner-filter effects at high concentrations of acceptor, we also used 2 mm  $\times$  2 mm cuvette or a laboratory-built sample holder with 0.1 mm path length. The detection path is at right angles to the excitation beam. Emission light passes through a diffracting spectrometer to isolate a single wavelength for detection with a photomultiplier tube (PMT) or to produce a spectrum detected by a charge-coupled detector (CCD). The PMT is used for time-resolved measurements, and the CCD is used to collect time-delayed emission spectra. The entrance to the spectrometer is equipped with a mechanical chopper synchronized to the laser pulse in order to block the entrance slit during and for 25  $\mu\text{s}$  after the laser pulse, thereby eliminating prompt fluorescence of the acceptor and any other short-lived background. Lifetime signals were fit to exponential functions using Table Curve software (Jandel Scientific). Spectral measurements were corrected for the wavelength sensitivity of the detection optics by using a standard lamp (Oriel) and further verified by comparison to a quinine sulfate standard spectrum (NIST reference). For measurements reported in Figure 4, the spectrometer was replaced with a high numerical aperture collection lens and a 546 nm  $\pm$  5 nm or 615 nm  $\pm$  7 nm interference filter for Tb and Eu, respectively. An Electron Tubes P30CWAD5-14 PMT was used in conjunction with these latter optics.

**Determination of Quantum Yield of Acceptors.** To measure  $Q_{\text{Ln}}$  via eq 5,  $Q_{\text{a}}$  must first be determined.  $Q_{\text{a}}$  was measured by standard methods, that is, by placing the acceptor alone in the solution used to determine  $Q_{\text{Ln}}$  and comparing its excited-state lifetime or the intensity of its emission to that of a known standard. For Tb<sup>3+</sup> the acceptors were fluorescein, QY = 0.93 in 1 N NaOH,<sup>9</sup> or 5-carboxytetramethylrhodamine (TMR), QY = 0.58 in 10 mM sodium phosphate buffer, pH 7.46, 80 mM NaCl;<sup>10</sup> for Eu<sup>3+</sup> the acceptor was SulfoRhodamine 101 in methanol, QY = 1, lifetime = 4.36 ns.<sup>11</sup>

**Determination of  $Q_{\text{overall}}$ .**  $Q_{\text{overall}}$  was determined by comparing the brightness of a lanthanide chelate to that of a known standard, where the concentrations of the chelate and standard were adjusted to give them the same absorbance at the excitation wavelength of 337 nm. For terbium, the standard was fluorescein in 1 N NaOH; for europium the standard was SulfoRhodamine 101 in ethanol. It was verified via nanosecond lifetime measurements (data not shown) that the quantum yield of fluorescein excited at 337 nm was the same as at 488 nm, that is, 0.93. For these measurements the mechanical chopper was turned off to enable detection of the prompt fluorescence from the standard.

## Results

### $Q_{\text{Ln}}$ 's of Terbium Chelates and Validity of the Method.

The results for diffusion-enhanced energy transfer between Tb-DTPA-cs124 and fluorescein are shown in Figure 2. The time-delayed emission spectra of donor-only and donor-acceptor samples are shown in the top graph, while the corresponding lifetimes are shown in the bottom graph. The lifetime of 1  $\mu\text{M}$  Tb-DTPA-cs124 is 1.56 ms (donor only, 1), and decreases to 1.33 ms (15% energy transfer, eq 3) in the presence of 0.2  $\mu\text{M}$  fluorescein (donor-acceptor, 2). The corresponding emission spectrum is shown as curve 2 in the top graph. The various intensities needed to determine  $Q_{\text{Ln}}$  via eq 5 are as follows.  $I_{\text{da}}$  is the area under the normalized donor emission (1).  $I_{\text{ad}}$  is the area difference between the spectrum 2 and spectrum 1. Addition of more fluorescein further decreases lifetime while simultaneously increasing the sensitized emission and energy transfer

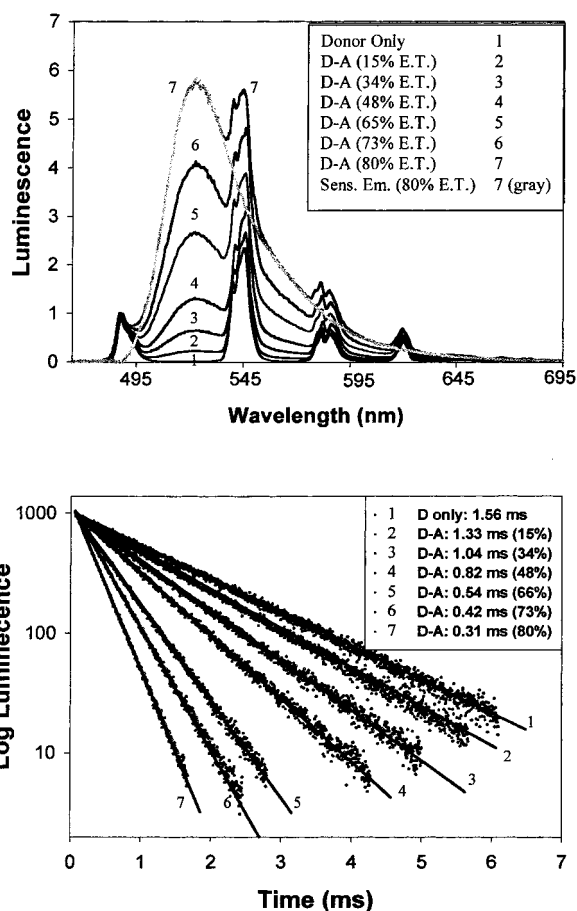


**Figure 2.** Diffusion-enhanced energy transfer from Tb-DTPA-cs124 to fluorescein. The top graph is the emission spectrum of the donor-only (Tb-DTPA-cs124) and donor-acceptor (Tb-DTPA-cs124 and fluorescein) mixture. The spectra are collected for 1 s with an entrance slit of 0.1 mm and a 300-groove/mm diffraction grating. Curve 1 is the emission of 1  $\mu\text{M}$  Tb-DTPA-cs124. Curves 2–7 represent the emission spectra of the mixture of 1  $\mu\text{M}$  Tb-DTPA-cs124 and fluorescein with increasing concentration from 0.2 to 4.5  $\mu\text{M}$  in 10 mM Mops, pH 8.35. The emission spectra are normalized at the 490 nm emission peak of Tb-DTPA-cs124. The gray curve in the top figure is the sensitized emission at 4.5  $\mu\text{M}$  acceptor concentration. It is obtained by subtracting the donor only emission (1) from the emission of donor-acceptor mixture (7). As expected, the shape of the sensitized emission is the same as an acceptor-only fluorescein spectra.  $I_{\text{da}}$  is the area under the donor-only emission curve, (1).  $I_{\text{ad}}$  is the area under the sensitized emission (gray curve). The bottom graph is the corresponding lifetime measurements for the samples used in the top graph. The numbering scheme was the same as the emission spectrum (top graph). Lifetime measurements were collected at either 490 or 520 nm, with 2  $\mu\text{s}$  resolution. (The lifetime is the same at all wavelengths). The data were fit to a single exponential (solid line), which showed no residual structure with  $r^2 = 0.999$ .

(curves 3–7). By substituting these results together with the quantum yield of fluorescein which we determined, 0.93, into eq 5, the quantum yield ( $Q_{\text{Ln}}$ ) of Tb<sup>3+</sup> in DTPA-cs124 was determined to be 0.486 (Table 1). We have also measured the quantum yield of Tb<sup>3+</sup> in DTPA-cs124 at various levels of energy transfer efficiency ranging from 15 to 80%, which were achieved by varying the concentration of the fluorescein acceptor from 0.2 to 4.5  $\mu\text{M}$  and keeping the donor concentration constant at 1  $\mu\text{M}$  (Figure 2). The results show the measured  $Q_{\text{Ln}}$ 's are independent of the energy transfer efficiency: the average is  $0.486 \pm 0.003$  for 17 samples with energy transfer efficiency ranging from 15 to 80% (Table 1). This demonstrates that any

(8) Xiao, M.; Selvin, P. R. *Rev. Sci. Instrum.* **1999**, *70*, 3877–3881.

(9) Weber, G.; Teale, F. W. J. *Trans. Faraday Soc.* **1957**, *53*, 646–655.

(10) Vamosi, G.; Gohlke, C.; Clegg, R. *Biophys. J.* **1996**, *71*, 972–994.

(11) Karstens, T.; Kobs, K. *J. Phys. Chem.* **1980**, *84*, 1871–1872.

**Table 1.** Terbium Lifetime, Quantum Yield and Rate Constant of Various Chelate Complexes in H<sub>2</sub>O and D<sub>2</sub>O

Tb chelate	$\tau$ (H <sub>2</sub> O) (ms)	quantum yield ( $Q_{Ln}$ ) in H <sub>2</sub> O $\pm$ SE <sup>a</sup>		rate constant (H <sub>2</sub> O) <sup>c</sup>		$\tau$ (D <sub>2</sub> O) (ms)	rate constant (D <sub>2</sub> O)		relative intensity of Tb chelate in H <sub>2</sub> O $\pm$ SE <sup>a</sup>	$Q_{Overall}$ of chelate complexes	$Q_{transfer}$ (%)
		measured with fluorescein as acceptor ( $n$ ) <sup>b</sup>	measured with TMR as acceptor ( $n$ )	average $Q_L$ in H <sub>2</sub> O	$K_{rad}$ (s <sup>-1</sup> )		$K_{nr}$ (s <sup>-1</sup> )	$K_{rad}$ (s <sup>-1</sup> )			
DTPA-cs124	1.55	0.486 $\pm$ 0.003 (17)	0.468 $\pm$ 0.006 (4)	0.482	311	2.63	311	69	1	0.324 $\pm$ 0.007 (8)	66.6%
TTHA-cs124	2.15	0.730 $\pm$ 0.016 (14)	0.741 $\pm$ 0.018 (4)	0.732	351	2.37	351	84	1.23	0.399 $\pm$ 0.006 (8)	54.7%
DOTA-cs124	1.54	0.436 $\pm$ 0.006 (5)	0.447 $\pm$ 0.004 (5)	0.442	287	2.61	287	96	0.99	0.320 $\pm$ 0.009 (8)	73.4%

<sup>a</sup> SE: standard error. <sup>b</sup> Experimental number. <sup>c</sup>  $K_{rad}$ : spontaneous radiative rate constant.  $K_{nr}$ : nonradiative rate.  $K_{nr} = (1 - Q)/Q(D_2O) = \tau(D_2O)/\tau(H_2O) * Q(H_2O)$ .

exchange interactions (contact terms) are either negligible or do not affect  $Q_{Ln}$ . In the same way, we determined  $Q_{Ln}$ 's of 0.730 for Tb-TTHA-cs124 and 0.436 for Tb-DOTA-cs124 using fluorescein as energy transfer acceptor (Table 1). These values are all independent of acceptor concentration, that is, independent of  $E$ .

To further test the effect of any exchange interactions on the measured quantum yields, we varied the ionic strength of the buffer, since it strongly affects contact terms when the donor and acceptor are charged.<sup>5</sup> Tb-DTPA-cs124 has a charge of  $-1$ , and fluorescein has a charge of  $-2$  under our experimental conditions. When the salt concentration was varied from zero to 1 M NaCl, energy transfer efficiency increased slightly, from 31 to 39% (0.5  $\mu$ M donor and acceptor), or from 65 to 73% (1  $\mu$ M donor and 2  $\mu$ M acceptor) (data not shown). The salt effect was more pronounced, as expected, for dinegative Tb-TTHA-cs124 and fluorescein. Energy transfer increased from 41 to 75% over the same salt range (1  $\mu$ M donor and 2  $\mu$ M acceptor; data not shown). However, in all cases the calculated  $Q_{Ln}$ 's are independent of ionic strength, affirming the validity of our measurements.

The  $Q_{Ln}$ 's of Tb-DTPA-cs124, Tb-TTHA-cs124, and Tb-DOTA-cs124 were also determined using a different energy transfer acceptor, 5-TMR. There is excellent agreement between these results and those determined with fluorescein (Table 1), again verifying the measurements' validity.

**$Q_{Ln}$ 's of Europium Chelate.** The quantum yields of Eu-chelate complexes (Eu-DTPA-cs124, Eu-TTHA-cs124, Eu-DOTA-cs124) were measured using SulfoRhodamine 101 as an energy transfer acceptor (Figure 3). The quantum yield of the acceptor (1  $\mu$ M), in the presence of the donor (1  $\mu$ M Eu-DOTA-cs124), was found to be 0.96 (4.20 vs 4.36 ns for SulfoRhodamine 101 in methanol; data not shown). At 1  $\mu$ M Eu-DOTA-cs124 and 0.25  $\mu$ M SulfoRhodamine 101 the donor emission lifetime decreased from 0.62 ms (curve 1) to 0.46 ms (curve 2), indicating 26% energy transfer. From these measurements and eq 5, the quantum yield of Eu-DOTA-cs124 was determined to be 0.137. Figure 3 also shows different energy transfer efficiencies arising from different acceptor concentrations. From these data we find that the calculated  $Q_{Ln}$  of Eu-DOTA-cs124 is independent of energy transfer efficiency (Table 2). Finally, using SulfoRhodamine 101 as an energy transfer acceptor, the quantum yields of Eu-DTPA-cs124 and Eu-TTHA-cs124 were measured to be 0.167 and 0.423, respectively (Table 2).

**Radiative and Nonradiative Rates and Quantum Yields in D<sub>2</sub>O.** With  $Q_{Ln}$  and  $\tau_d$  determined in H<sub>2</sub>O, radiative and nonradiative decay rates for the lanthanides in aqueous solutions were calculated via eq 6 for each chelate. By measuring  $\tau_d$  in D<sub>2</sub>O and assuming that the radiative rates do not to change in going from H<sub>2</sub>O to D<sub>2</sub>O,  $Q_{Ln}$  in D<sub>2</sub>O was then calculated. This assumption is justified since the spontaneous emission rate is expected to be a function of chelate symmetry, which is unaffected by the replacement of H<sub>2</sub>O by D<sub>2</sub>O. The measured values are listed in Tables 1 and 2.

**Overall and Transfer Quantum Yield.** Tables 1 and 2 report the overall quantum yields for Tb and Eu in the polyaminocarboxylate chelates (Figure 1).  $Q_{Overall}$  ranges from 0.32 to 0.4 for Tb in H<sub>2</sub>O (0.44 to 0.55 in D<sub>2</sub>O), and from 0.06 to 0.28 for Eu in H<sub>2</sub>O (0.21 to 0.42 in D<sub>2</sub>O). The highest previously reported overall quantum yield for a lanthanide complex is 0.7 (with Eu), although this required the use of nonaqueous environment.<sup>12</sup> The highest previously reported value in H<sub>2</sub>O

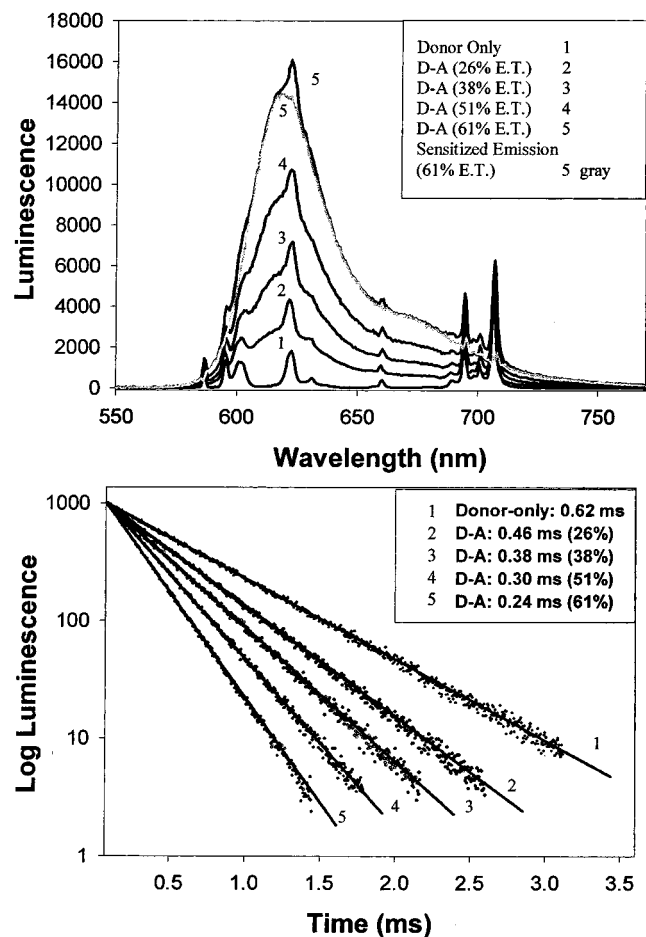


**Figure 3.** Typical experimental results of diffusion-enhanced energy transfer from Eu-DOTA-cs124 to SulfoRhodamine 101. The top graph is the normalized emission spectrum of the donor only (Eu-DOTA) and donor-acceptor (Eu-DOTA and SulfoRhodamine 101) mixture with the same spectrometer settings as Figure 2. Curve 1 is the donor-only. Curves 2–5 are the normalized donor-acceptor emission. They represent emission curves of the mixtures of 1  $\mu\text{M}$  Eu-DTPA with increasing concentration of SulfoRhodamine from 0.2 to 1  $\mu\text{M}$  in 10 mM MOPS buffer (pH 7.0). The gray curve (5) is the sensitized emission of the sample with 61% energy transfer, which is the difference of curves 5 and 1. The bottom graph is the corresponding lifetime data, with the same numbering scheme. The lifetimes were collected at either 590 or 700 nm (lifetimes are the same at all wavelengths) with 2  $\mu\text{s}$  resolution. Data were fit to single exponentials (solid lines), which showed no residual structure with  $r^2 = 0.999$ .

is 0.58 for Tb.<sup>13</sup> From eq 1, the internal transfer efficiency can be inferred.  $Q_{\text{transfer}}$  ranges from 41 to 66% for Eu<sup>3+</sup> and from 55 to 73% for Tb<sup>3+</sup>.

**Detection Limits.** Figure 4 is a standard titration curve showing that the detection limit of free Tb-DTPA-cs124 is  $1.0 \times 10^{-13}$  M and free Eu-TTHA-cs124 is  $4 \times 10^{-13}$  M. The detection limit for chelate bound to a biomolecule will likely be biomolecule specific, but for DTPA-cs124, the intensity upon conjugation ranges from unchanged to 10 $\times$  lower than that of free chelate.<sup>14,15</sup>

**Quantum Yield of Acceptor Fluorophores.** Once  $Q_{\text{Ln}}$  is known,  $Q_{\text{a}}$  of many common fluorophores can readily be

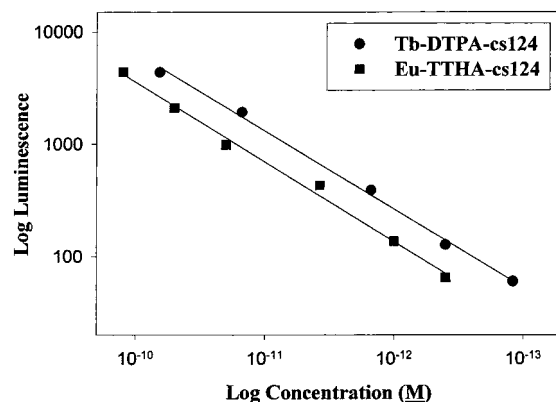


**Figure 4.** Standard curve for determining detection limits. Sample volume was 100  $\mu\text{L}$ . Counts are for 2  $\mu\text{s}$  bin, 1 ms after the laser pulse, 1000 pulses total.

determined via eq 5. The only limitation is that the fluorophore must be able to act as an energy transfer acceptor for a lanthanide chelate, although, given the wide spectral range of terbium and europium, most visible and red (e.g. 600–800 nm emission) dyes fall into this category. We measured the quantum yields of (unbound) Cy5 and Cy5.5, two far-red dyes, using three different donors: Eu-DTPA-cs124, Eu-DOTA-cs124, and Eu-TTHA-cs124. We found quantum yields of 0.4 for Cy5 and 0.3 for Cy5.5 (Table 2). The former result is somewhat higher than previously reported.<sup>16</sup>

## Discussion

A number of efforts have been made to measure the quantum yield,  $Q_{\text{Ln}}$ , of lanthanides in solution. With one exception,<sup>17</sup> these measurements were made by the direct excitation method - - directly exciting the lanthanide and comparing the emitted intensity with the intensity of a fluorophore of known quantum yield. This method is problematic because of the weak absorption and emission of lanthanide chelates in water and because it often requires comparing absolute intensities of a sample and reference excited or emitting at very different wavelengths. These methods are also not able to measure the  $Q_{\text{transfer}}$  for sensitizer-chelate complexes. The method presented here is simple and robust because  $Q_{\text{Ln}}$  can be determined on a single sample by comparing lifetime and spectral measurements. As seen in Tables 1 and 2, the precision in the measurements of  $Q_{\text{Ln}}$  is excellent. The accuracy of  $Q_{\text{Ln}}$  depends on how well  $Q_{\text{a}}$  is known, but  $Q_{\text{a}}$  has been extensively studied for fluorescein and rhodamine. Indeed,  $Q_{\text{Ln}}$ 's measured using both acceptors agree very well with each other (Tables 1 and 2), indicating the accuracy is very good such that the error is probably less than 5–10%. In addition,  $Q_{\text{overall}}$  can be measured relatively simply and reliably by exciting the lanthanide sample and the reference at a single wavelength, and choosing a reference that emits in a wavelength range similar to that of the lanthanide.

In this way we have characterized the photophysical steps in the excitation and emission process of lanthanide chelates. We find the transfer of energy from antenna to lanthanide is surprisingly high, on the order of or greater than 50%, and the probability that the lanthanide will then emit a photon ( $Q_{\text{Ln}}$ ) is also quite high, ranging from 14 to over 80%, depending on choice of lanthanide, chelate, and solvent (H<sub>2</sub>O or D<sub>2</sub>O). The product of these two terms is the overall quantum yield, which

(12) Hemmilä, I.; Mukkala, V.-M.; Takalo, H. J. *J. Alloys Compd.* **1997**, *249*, 158–162.

(13) Latva, M.; Takalo, H.; Mukkala, V.-M.; Matachescu, C.; Rodriguez-Ubis, J. C.; Kankare, J. *J. Lumin.* **1997**, *75*, 149–169.

(14) Chen, J.; Selvin, P. R. *Bioconjugate Chem.* **1999**, *10*, 311–315.

(15) Li, M.; Selvin, P. R. *Bioconjugate Chem.* **1997**, *8*, 127–132.

(16) Mujumdar, R. B.; Ernst, L. A.; Mujumdar, S. R.; Lewis, C. J.; Waggoner, A. S. *Bioconjugate Chem.* **1993**, *4*, 105–111.

(17) Drexhage, K. H. *Sci. Am.* **1970**, *222*, 108–119.

**Table 2.** Europium Lifetime and Quantum Yield in Various Chelates Complex in H<sub>2</sub>O and D<sub>2</sub>O

europium complex	$\tau$ (H <sub>2</sub> O) (ms)	quantum yield ( $Q_{Ln}$ ) of Eu in H <sub>2</sub> O $\pm$ SE <sup>a</sup>		rate constant (H <sub>2</sub> O) <sup>c</sup>		$\tau$ (D <sub>2</sub> O) (ms)	quantum yield ( $Q_{Ln}$ ) in D <sub>2</sub> O <sup>d</sup>	rate constant (D <sub>2</sub> O)		relative intensity of lanthanide chelate complexes in H <sub>2</sub> O $\pm$ SE <sup>a</sup>	$Q_{overall}$ of chelate complexes	$Q_{transfer}$ (%)	QY of Cy5 <sup>e</sup>	QY of Cy5.5 <sup>f</sup>
		measured with SR101 as acceptor (n) <sup>b</sup>	measured with Cy5 as acceptor (n)	$K_{rad}$ (s <sup>-1</sup> )	$K_{nr}$ (s <sup>-1</sup> )			$K_{rad}$ (s <sup>-1</sup> )	$K_{nr}$ (s <sup>-1</sup> )					
DTPA-cs124	0.62	0.167 $\pm$ 0.004 (9)	0.419 $\times Q_A^c \pm 0.004$ (4)	269	1348	2.42	0.652	269	144	1	0.099 $\pm$ 0.002 (8)	59.1%	0.400 $\pm$ 0.012(4)	0.300 $\pm$ 0.008 (3)
TTHA-cs124	1.19	0.423 $\pm$ 0.004 (12)	1.08 $\times Q_A \pm 0.022$ (10)	355	484	1.79	0.636	355	203	2.84	0.280 $\pm$ 0.006 (8)	66.3%	0.392 $\pm$ 0.006 (4)	0.310 $\pm$ 0.01 (3)
DOTA-cs124	0.62	0.137 $\pm$ 0.006 (4)	0.329 $\times Q_A \pm 0.005$ (4)	220	1386	2.25	0.497	220	221	0.57	0.057 $\pm$ 0.0002 (8)	41.2%	0.416 $\pm$ 0.009 (4)	0.315 $\pm$ 0.009 (3)

<sup>a</sup> SE: Standard error. <sup>b</sup> Experimental number. <sup>c</sup> Quantum Yield of Acceptor (Cy5). <sup>d</sup> Quantum yield of Cy5 is calculated by comparing columns 2 and 3. <sup>e</sup>  $K_{rad}$ : Spontaneous radiative rate constant.  $K_{nr}$ : nonradiative rate.  $K_{rad} = \tau/Q$  (s<sup>-1</sup>),  $K_{nr} = (1 - Q)K_{rad}/Q$ . <sup>f</sup>  $Q(D_2O) = \tau(D_2O)/\tau(H_2O) * Q(H_2O)$ .

ranges from 10 to over 50%. These values are generally many orders of magnitude greater than phosphorescent organic probes.

**Implications for Lanthanide Photophysics.** Horrocks and Sudnik, in their seminal work, showed that by measuring the relative total decay rates (radiative plus nonradiative) of lanthanides in H<sub>2</sub>O and D<sub>2</sub>O, the number of waters coordinated to the lanthanide could be determined.<sup>18</sup> They were not, however, able to determine the individual  $k_{rad}$  and  $k_{nr}$ . This is now possible (Tables 1 and 2). One finding is that  $k_{rad}$  increases with chelate asymmetry: TTHA is the most asymmetrical and has the fastest rate, DTPA is next, and DOTA is the most symmetrical and has the lowest rates for Tb and Eu. (For a discussion of chelate symmetry, see refs 4 and 19.) This trend is expected if emission primarily arises from electric dipole (ED) transitions, as opposed to magnetic dipole (MD) transitions, which would have the opposite correlation between radiative rates and asymmetry. (See also ref 17 for more detailed discussion of MD vs ED.) The predominance of ED transitions has important ramifications for their use as energy transfer donors (see below). Further experiments can more rigorously test the relative contributions of these terms as a function of emission wavelength.<sup>17</sup>

$k_{nr}$  also can be analyzed. The nonradiative rates are a function of chelate and H<sub>2</sub>O versus D<sub>2</sub>O (Tables 1 and 2). In all cases quenching decreases when substituting D<sub>2</sub>O for H<sub>2</sub>O, as expected. It is well-known that O-H, bound to the primary coordination sphere of Eu or Tb, leads to quenching, whereas O-D quenching is much smaller.<sup>18</sup> Indeed, the exclusion of H<sub>2</sub>O from the primary coordination sphere is one of the central tasks of the chelate. With TTHA, 0.2 water molecules remain, whereas with DTPA and DOTA 1.1 H<sub>2</sub>O molecules are bound. Hence, in aqueous solutions, the nonradiative rates for Eu and Tb with TTHA-cs124 are significantly lower than DTPA-cs124 and DOTA-cs124. Correspondingly, the quantum yields are higher in TTHA in H<sub>2</sub>O-solutions. However, the  $Q_{Ln}$ 's are not unity even in D<sub>2</sub>O solutions (0.5–0.8), implying that the chelate (likely N-H and C-H vibrations<sup>20</sup>) introduces modest nonradiative pathways. (We have previously shown that the sensitizer does not lead to nonradiative de-excitation pathways for the lanthanide<sup>4,21</sup>). A detailed comparison between different chelates indicates that the nonradiative pathways are slightly greater for chelates containing coordinating nitrogens than for chelates with coordinating carboxylate groups.

**Implications for Detection Limits.** The relatively high overall quantum yields, combined with the reasonable absorption cross-section of the antenna ( $10^4$  M<sup>-1</sup> cm<sup>-1</sup> at 337 nm<sup>4</sup>), enable high sensitivity ( $\approx 10^{-13}$  M detection limit) when time-resolved and wavelength-discriminated detection is used. This high detection sensitivity has given lanthanides broad applicability, particularly in bioassays such as high throughput screening or imaging of clinical samples, where background fluorescence often limits sensitivity of conventional fluorophores.<sup>1,3</sup> For example, under such conditions, improvements in signal/background of 1000-fold can be achieved using lanthanide labels combined with temporal and spectral discrimination against background.<sup>22</sup> Furthermore, the large Stokes' shift and water-

(18) Horrocks, W. D., Jr.; Sudnick, D. R. *J. Am. Chem. Soc.* **1979**, *101*, 334–350 and references therein.

(19) Bunzli, J.-C. G. Luminescent Probes. In *Lanthanide Probes in Life, Chemical and Earth Sciences, Theory and Practice*; Bunzli, J.-C. G., Choppin, G. R., Eds.; Elsevier: New York, 1989; pp 219–293 and references therein.

(20) Dickens, R. S.; Parker, D.; Desousa, A. S.; Williams, J. A. G. *Chemical Commun.* **1996**, *6*, 697–698.

(21) Snyder, G.; Selvin, P. R. *Photophysical Properties of Luminescent Lanthanide Chelates*; Biophysical Soc. Meeting, Kansas City, 1998.

soluble nature of lanthanide chelates have allowed over 100 chelates to be attached via a polylysine tail to a single biomolecule while retaining biological activity and yielding a linear increase in signal.<sup>23,24</sup> Hence, detection limits of  $10^{-15}$  M for lanthanide-tagged biomolecules are expected.

#### Implications for Lanthanides As Energy Transfer Donors.

Lanthanides have also been shown to be excellent donors in resonance energy transfer measurements.<sup>1-3,18</sup> However, until now, the quantum yield ( $Q_{Ln}$ ) has been a poorly determined, yet important, parameter in these measurements. The distance,  $R$ , inferred from energy transfer experiments via donor lifetime or intensity measurements, depends on knowing the donor ( $Q_{Ln}$ ) quantum yield:  $R \propto Q_{Ln}^{1/6}$ . We and others have explicitly or implicitly assumed that  $Q_{Ln}$  is unity in  $D_2O$ , and here we show that this assumption is not rigorously correct, although the errors introduced are relatively small. In  $H_2O$  solutions, the distance errors introduced by this assumption are <4% for Tb-DTPA-cs124 and <7% for Eu-DTPA-cs124. It should be noted that the  $Q_{Ln}$  measured here arises from both electric dipole and magnetic dipole transitions, and only the former contributes to energy transfer<sup>7,25</sup> (but see above section, Lanthanide Photo-physics).

**Implications for Further Improvement in Lanthanide Chelates.** Our results support the notion that polyaminocarboxylate chelates are effective at shielding the lanthanide from the quenching effects of water and enable reasonably efficient transfer of energy from an antenna molecule to the lanthanide, particularly for Tb. Most importantly, the ability to dissect the energy transfer and luminescence process should enable a comparison and optimization of different chelates. For example, it has previously been noted that Tb and Eu in DOTA have a surprisingly short lifetime compared to that in DTPA and TTHA, but it was not possible to determine if this was due to differences in radiative or nonradiative rates.<sup>4</sup> Having explicitly measured  $k_{nr}$ , we can now conclude that the difference is indeed due to additional nonradiative pathways in DOTA. The ability to

measure, and ultimately optimize,  $Q_{transfer}$  is also important. A larger  $Q_{transfer}$  increases the brightness of the lanthanide complex and is expected to make the antenna more photostable since energy transfer to the lanthanide competes with photochemical destruction. The effect of parameters that likely affect  $Q_{transfer}$ , such as the distance and number of bonds between antenna and lanthanide,<sup>26</sup> can now be systematically studied.

**Implications of  $Q_a$  for Far-Red Dyes.** Red-emitting probes (e.g., >650 nm) are of interest because autofluorescence decreases with increasing wavelength, and hence red dyes lead to enhanced sensitivity.<sup>27,28</sup> These dyes have also recently been used in energy transfer measurements to measure large distances.<sup>29</sup> However, evaluating their quantum yields has been difficult, in part because few good quantum yield standards exist in the 650–800 nm spectral range.<sup>30-32</sup> We find a value of 0.4 for Cy5, somewhat higher than the 0.28 value previously reported, and 0.3 for Cy5.5, in good agreement with previously published numbers. The accuracy of these numbers depends on the accuracy of  $Q_{Ln}$ , as discussed above. We believe these two dyes can now serve as standards for comparing and characterizing far-red dyes. The higher value for Cy5 also implies that it is an excellent donor in fluorescence energy transfer experiments, with an  $R_0$  exceeding 85 Å when used with Cy5.5 as an acceptor.<sup>29</sup>

**Acknowledgment.** This work was supported by NIH Grant AR44420 and by Amersham-Pharmacia Biotech. We thank the Laboratory of Fluorescence Dynamics for the use of their nanosecond lifetime instrument.

JA0031669

(26) Kirk, W. R.; Wessels, W. S.; Prendergast, F. G. *J. Phys. Chem.* **1993**, *97*, 10326–10340.

(27) Yu, H.; Ernst, L.; Wagner, M.; Waggoner, A. *Nucleic Acids Res.* **1992**, *20*, 83–88.

(28) Sauer, M.; Zander, C.; Müller, R.; Ullrich, B.; Drexhage, K. H.; Kaul, S.; Wolfrum, J. *App. Phys. B* **1997**, *65*, 427.

(29) Schobel, U.; Egelhaaf, H.-J.; Brecht, A.; Oelkrug, D.; Gauglitz, G. *Bioconjugate Chem.* **1999**, *10*, 1107–1114.

(30) Lakowicz, J. R. *Principles of Fluorescence*, 2nd ed.; Kluwer Academic: New York, 1999.

(31) Fonda, H. N.; Gilbert, J. V.; Cormier, R. A.; Sprague, J. R.; Kamioka, K.; Connolly, J. S. *J. Phys. Chem.* **1993**, *97*, 7024–7033.

(32) Isak, S. J.; Eyring, E. M. *J. Phys. Chem.* **1992**, *96*, 1738–1742.

(22) Seveus, L.; Vaisala, M.; Hemmila, I.; Kojola, H.; Roomans, G. M.; Soini, E. *Microsc. Res. Tech.* **1994**, *28*, 149–154.

(23) Canfi, A.; Bailey, M. P.; Rocks, B. F. *Analyst* **1989**, *114*, 1908–1911.

(24) Moronne, M. M. *Ultramicroscopy* **1999**, *77*, 23–36.

(25) Dexter, D. L. *J. Chem. Phys.* **1953**, *21*, 836–850.